Nature Environment and Pollution Technology
An International Quarterly Scientific Journal

ISSN: 0972-6268 | Vol. 13 | No. 4 | pp. 669-676 | 2014

Original Research Paper

The Influence of Spatial Resolution on the Prediction of Soil Organic Matter Distribution in a Mollisol Watershed of Northeast China

Shaoliang Zhang and Xingyi Zhang*
College of Resource and Environment, Northeast Agricultural University, 59 Mu Cai Street, Harbin 150030, PR China
*Northeast Institute of Geography and Agroecology, Chinese Academy of Sciences, 138 Haping Road, Harbin 150081, PR China
Corresponding author: Shaoliang Zhang

Nat. Env. & Poll. Tech.
Website: www.neptjournal.com

Received: 2-12-2013
Accepted: 16-1-2014

Key Words:
Soil organic matter
Sampling resolution
Spatial distribution
Geostatistics
Landscape indicator

ABSTRACT

Geostatistics, traditional statistics and landscape indicators were used to analyse the influence of sampling resolution on the prediction of spatial variability of soil organic matter (SOM) in a typical Mollisol of northeast China. Gaussian models were recognized as the best to predict SOM spatial distribution in all resolution groups. Spatial autocorrelations as influenced by structure factors were moderate for groups 0.025, 0.037b, 0.074a, 0.074c and 0.074d, and strong for 0.015, 0.037a, 0.074b and 0.074e. The relatively shorter autocorrelation distances (A_0) in data groups were all close to 7 km. Means and standard deviation (SD) of 0.025 resolution was close to 0.015. TA (Total area), LPI (Largest patch index) and COHESION (Patch cohesion index) were similar between resolutions 0.015 and 0.025. Generally, a sample-grid ≤ 0.025 km^2 was recognized as a better resolution to predict SOM spatial variability by ordinary kriging interpolation if a sample-grid method was adopted in the black soil region of northeast China. The accurate prediction of soil nutrient heterogeneity by interpolations (Geostatistics) is mainly determined by the representative of soil sampling which should reflect through resolution the entire environmental factors in the research area.

INTRODUCTION

Generally, it is difficult to predict accurately the soil nutrient distribution in an agricultural watershed, because the spatial heterogeneity of soil nutrients in the area is affected by many complicated factors (Lal 1998, Huang 2000, Barton et al. 2004, Atreya et al. 2008). One of the primary factors affecting nutrient distribution is physical movement of the soil, as runoff from upslope areas carries topsoil to lower slope positions, thus altering the spatial distribution of soil and water, and affecting soil nutrient content in both affected areas (Balasundram et al. 2006, Noorbakhsh et al. 2008, Verity & Anderson 1990, Moulin et al. 1994). It is apparent that the steepness of a slope influences the intensity of soil erosion and thus affecting soil nutrient distribution in the field, but soil erosion as affected by slope also varies according to the type of soil (Agassi et al. 1990, Walson & Laflen 1986, Liu et al. 2006, Morgan 2005). Slope aspect can also be important in affecting nutrient distribution, as equatorial slopes tend to be dryer than polar-facing ones because they have greater evapo-transpiration rates (Rundel 1981), while the amount of rainfall, and thus runoff, tends to be greater on a windward slope than on the leeward side (Agassi et al. 1990). Studies of the effect of land management on nutrients has shown that cultivation generally increases the potential for soil erosion due to the breakdown of soil aggregates and reduction of soil cohesion, and thus decreasing soil nutrient content in the profile (Horn et al. 1995, Walson & Laflen 1986). By extension, since cross-slope tillage reduces soil loss compared to down-slope tillage (Voroney et al. 1981, Van Doren et al. 1950), it can be expected that nutrient levels would also be less affected. It is also reported that soil nutrient content varies considerably under different crops (Huang 2000, Gardner & Gerrard 2003), and that generally continuous corn (*Zea mays* L.) and corn-soybean (*Glycine max* L.) rotations do not result in a significant accumulation of soil organic carbon (SOC) (West & Post 2002). Fertilizer application rates can also affect soil nutrient content dynamics in the field (Lal 2004, Liu et al. 2006). Thus, soil nutrient heterogeneity is complexly influenced by so many factors, and how to improve the accuracy of prediction was focused on by researchers in recent years.

Generally, geostatistics, linear models, neural networks, regression trees, fuzzy systems and other analytical procedures have been used to analyse soil nutrient distributions and are considered good tools for use in understanding nutrient dynamics in the field (Zhang et al. 2007, Liu et al. 2006, DeBusk et al. 1994, Park & Lekm 2002). Although the sophisticated analytical techniques available and the recognition of the importance of understanding nutrient variability, but soil nutrient variability with respect to sampling resolution is still poorly understood (Silveira et al. 2009, Gallardo 2003, Zhang et al. 2007, Zhang et al. 2011). Currently, the spatial pattern and ecological flow process are affected by sampling resolution is well known in landscape ecology (Fu et al. 2011, Forman 1995). Resolution refers to the resolution of the data, i.e., the area represented by each data unit. For example, a fine-resolution map might organize information into l ha units, whereas a map with an order of magnitude coarser resolution would have information organized into l0 ha units (Turner et al. 1989). Currently, geostatistics, a popular and powerful approach, along with conventional laboratory analysis is still used to predict soil nutrient distribution in soils because the prediction is relatively accurate, although the methods require a fairly dense sampling network and incur a high cost (Fu et al. 2013, Sauer et al. 2006, Wu et al. 2003, Liu et al. 2013). To understand soil nutrient spatial variability by geostatistics method, the sample-grid method and sample-random method are usually adopted for soil sampling, and sample points should be distributed uniformly in space, also the data need to fit to a normal distribution and second order stationary hypothesis (Zhang et al. 2007, 2011). However, there is always a coincident spatial distribution of soil nutrients predicted by geostatistics with the sample random method or sample-grid method under different resolutions. Despite the sample points distribute uniformly, and the data fit to a normal distribution and second order stationary hypothesis, the regression also shows the estimated value fits well with the actual value. In this study, in order to determine the effect of sampling resolution on the prediction of soil nutrient distribution, soil samples were collected in 2007 in a 6.55 km^2 region of typical Mollisol soils. Using Ordinary Kriging procedures and landscape indictor methods to describe the spatial variability of the soil organic matter (SOM), also the spatial distributions were compared among the four resolutions and among different data groups within the same resolution (Yost et al. 1982, Oliver 1987, Debusk et al. 1994).

MATERIALS AND METHODS

The 6.55 square kilometre (1.57 km × 4.17 km) study area is located in Guangrong village (47.21-47.23°N, 126.50-126.51°E) in Hailun city, Heilongjiang province, Northeast China (Fig. 1). The area falls in the north temperate zone and has a continental monsoon climate of cold and arid weather in winter and hot and rainy conditions in summer. Average annual precipitation is 530 mm, with 65% falling in June, July and August. Average precipitation from March to October in the 2002-2008 period was 472.3 mm. The average annual temperature is 1.5°C and annual sunshine averages between 2600 and 2800 hours. Total annual solar radiation is 113 MJ cm^{-2} and annual average available accumulated temperature (≥ 10°C) is 2450°C. The prevailing wind is from the north-west in winter and spring and from the south-west in summer (Soil Survey Service of Hailun 1985). Formation of soils in the study area began during the Quaternary period on loess deposits under natural grasses, and now have a rich, dark organic horizon and are classified as Mollisols (Zhang et al. 2007). These soils have a silty clay loam texture (Table 1), and most slopes are inclined at less than 5°, but are over 200 meters in length.

SOIL SAMPLE COLLECTION AND MEASUREMENT

Four hundred forty eight soil samples were collected in a sample-grid method from a depth of 0-20 cm in the autumn of 2007 after harvest (Fig. 2) (Li et al. 2008). Each soil sample was comprised of a mixture of six cores taken randomly from within a 20 m^2 plot. Samples were air-dried and sieved at 0.25 mm for analysing soil organic matter (SOM). SOM was measured using a Vario ELIII.

Sample points were classified into five data groups (G1, G2, G3, G4 and G5) randomly at first, to ensure that the data should have a close to normal distribution or close to normal distribution after transformation by the logarithm method in each group. Then the five data groups were regrouped into nine data groups of 0.015 (G1+G2+G3 +G4+G5), 0.025 (G1+G3+G5), 0.037a (G1+G4), 0.037b (G2+G5), 0.074a (G1), 0.074b (G2), 0.074c (G3), 0.074d (G4) and 0.074e (G5) (Table 2) again within no repeat sample in the new data group of the resolution 0.015 km^2, 0.025 km^2, 0.037 km^2, or 0.074 km^2, respectively.

KRING ANALYSIS

The spatial distribution of SOM was determined by a geostatistical analysis module using ArcGIS10 (ESRI 2010). Semivariograms were used in an autocorrelation analysis in order to evaluate the spatial dependence of the values, and

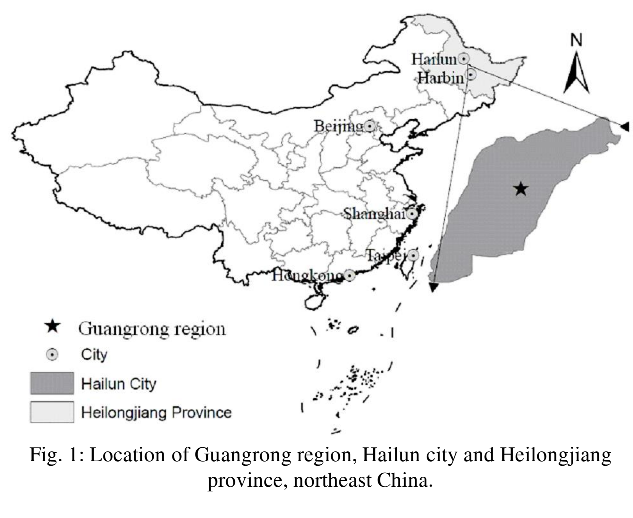

Fig. 1: Location of Guangrong region, Hailun city and Heilongjiang province, northeast China.

Table 1: Soil physical and chemical properties in the watershed.

Soil Depth	Organic Matter	Bulk Density Content	Total Porosity	Field Capacity	Saturated Water	Withering Moisture
cm	g/kg	g/cm	%	w/w, %	w/w, %	w/w, %
0-20	42.1	1.27	52.1	24.4	42.3	12.1
20-40	28.4	1.19	55.1	24.4	44.2	13.4
40-60	18.6	1.21	54.3	23.4	43.6	14.2

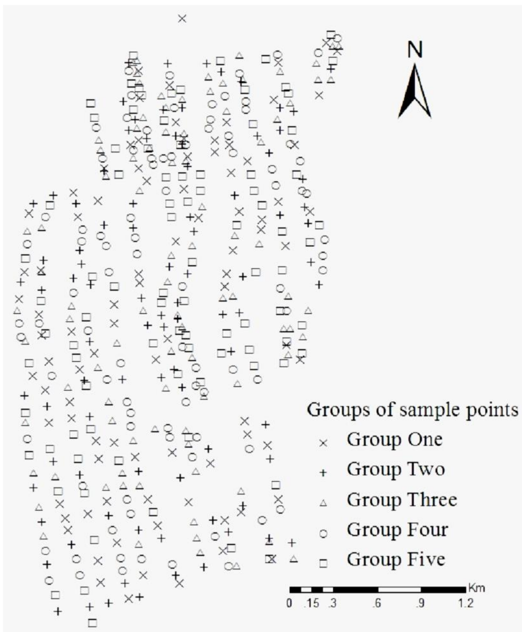

Fig. 2: Distribution of sample sites and groups classification in the study area.

best-fit models were optimized to predict SOM (Oliver et al. 2000). Semivariograms were calculated according to the formula: $\gamma(h) = 1/2N(h)\ \Sigma[z(x_i + h) - z(x_i)]^2$ (Isaaks & Srivastava 1989), where $\gamma(h)$ is the experimental semivariogram value at distance interval h, $N(h)$ is the number of sample pairs within the distance interval h and $z(x_i)$, $z(x_i + h)$ is the sample value at two points separated by the distance interval h. The ordinary Kriging algorithm was used to create an interpolated grid for development of isarithmic maps of SOM. Since the distribution of SOM values based on the 448 sample points were transformed by the logarithm method to normally distributed in nine groups (0.015, 0.025, 0.037a, 0.037b, 0.074a, 0.074b, 0.074c, 0.074d and 0.074e), Kurtosis and skewness values were then used to determine the goodness of fit to a normal distribution. Kurtosis values of SOM were close to 3, and skewness values were close to 0. Anisotropic analysis indicated that the average semivariance of SOM between 0° (north-south) and 90° (east-west), or between 45° (northeast-southwest) and 135° (southeast-northwest) were closer at the same separation distances, and $K(h)$ (the ratio of average semivariance 0° to 90°, or 45° to 135°) values were close to "1" in groups. By this measure, SOM can be considered as isotropic in the study area at the group level, and the results were reported (Zhang et al. 2011). The coefficient of determination provides an indication of how well a model fits variogram data, but this value does not serve as well as the residual sum of squares (RSS) value for best-fit calculations involving changes in a model parameter. The lower the RSS, the better the model fits (Table 2). A Gaussian model was selected as the best for predicting SOM in the nine groups, and cross-validation method with R^2 (Regression coefficient) showed the estimated values fit well with the actual values.

The Gaussian isotropic model can be depicted as follows:

$$\gamma(h) = C_0 + C\left[1 - \exp(-h^2 / A_0^{\ 2})\right]$$

Where h = lag interval, C_0 = nugget variance ≥ 0, C = structure variance $\geq C_0$, and A_0 = range parameter.

After interpolation by ordinary Kriging in nine groups, SOM values were classified into five classes (very insufficient, insufficient, sufficient, rich and very rich are represented by <30 g/kg, 30-40 g/kg, 40-50 g/kg, 50-60 g/kg, >60 g/kg, respectively) according to the SOM classification system of Heilongjiang province.

LANDSCAPE INDICATORS

Number of patches (NP): Equals the number of patches having the same class metrics.

Total area (TA): Equals the total area of all patches having the same class metrics.

Total perimeter (TP): Equals the perimeter of all patches having the same class metrics.

Largest patch index (LPI): Equals the area of the largest patch divided by total area having the same class metrics, multiplied by 100 (to convert to a percentage).

Shape index (SHAPE-MN): It corrects for the size problem of the perimeter-area ratio index by adjusting for a square (or almost square) standard and, as a result, is the simplest and perhaps most straightforward measure of overall shape complexity.

$$SHAPE = \frac{P_{ij}}{\min\ p_{ij}}$$

p_{ij} equals the perimeter (m) of patch ij.

Patch cohesion index (COHESION): It measures the physi-

Table 2: Geostatistical parameters in data groups.

Group name	Resolution (km^2) (448)	Resolution (m×m)	Data group	C_0	C_0+C	A_0(km)	C_0/C_0+C	Model	RMSE	R^2
0.015	0.015 (269)	122×122	1,2,3,4,5	0.035	0.160	7.1	0.22	Gaussian	2.6E-05	1.02
0.025	0.025 (179)	158×158	1,3,5	0.147	0.294	7.1	0.50	Gaussian	8.0E-04	0.89
0.037a	0.037 (179)	192×192	1,4	0.036	0.272	6.9	0.13	Gaussian	2.6E-04	0.88
0.037b	0.037 (90)	192×192	2,5	0.162	0.395	7.1	0.41	Gaussian	4.8E-04	0.69
0.074a	0.074 (90)	272×272	1	0.045	0.090	7.1	0.50	Gaussian	1.6E-04	0.66
0.074b	0.074 (90)	272×272	2	0.047	0.277	7.1	0.17	Gaussian	3.3E-04	0.91
0.074c	0.074 (90)	272×272	3	0.061	0.138	7.1	0.45	Gaussian	2.9E-04	0.76
0.074d	0.074 (89)	272×272	4	0.101	0.202	7.1	0.50	Gaussian	1.1E-03	0.82
0.074e	0.074 (89)	272×272	5	0.082	0.518	6.7	0.16	Gaussian	6.5E-04	0.89

R^2 (Regression coefficient)

cal connectedness of the corresponding patch type. Patch cohesion increases as the patch type becomes more clumped or aggregated in its distribution; hence, more physically connected.

$$COHESION = \left[1 - \frac{\sum_{j=1}^{n} p_{ij}}{\sum_{j=1}^{n} p_{ij}\sqrt{a_{ij}}}\right] \cdot \left[1 - \frac{1}{\sqrt{Z}}\right]^{-1} \cdot (100)$$

p_{ij} equals the perimeter of patch ij in terms of number of cell surfaces. a_{ij} equals the area of patch ij in terms of number of cells. Z equals the total number of cells in the landscape. Landscape indicators were calculated by the software Fragstats 3.0 (Mc Garigal et al. 2012).

RESULTS

SOM spatial distribution under sample-grids of 0.015 km^2 and 0.025 km^2: SOM spatial distribution trends were similar between the 0.025 and 0.015 resolutions, and SOM was higher in most of the areas in the west, then declined in an easterly direction, with some variations (Fig. 3). The TA of 40-50 g/kg in 0.015 or 0.025 was largest, and the areas of 60 g/kg>SOM> 40 g/kg accounted for 88% and 87% of the study area in 0.015 and 0.025, respectively. Both NP and TP for 40-50 g/kg in 0.015 and 50-60 g/kg in 0.025 were the largest classes. Both LPI and COHESION for 40-50 g/kg were the largest in the 0.025 and 0.015 classes. SHAPE-MN for 50-60 g/kg in 0.015 and 40-50 g/kg in 0.025 were largest among classes of SOM content.

SOM spatial distribution under sample-grid of 0.037 km^2: SOM spatial distribution in the 0.037 km^2 resolution (Fig. 4a and 4b) differed from that of 0.015 km^2, and was also different between 0.037a and 0.037b. SOM was higher in the southwest, northwest and middle area of the western region in 0.037a, while SOM was higher in northeast and middle area of the western region in 0.037b (Fig. 4). The TA of 40-50 g/kg was largest in the 0.037a group and 1.5 times larger than that in 0.015. As well, 50-60 g/kg was largest in the 0.037b group and covered 61.5% of the area of 0.015. The area of 60 g/kg>SOM> 40 g/kg accounted for 96% and 99% of the study area in 0.037a and 0.037b, respectively. Both the NP and TP of 40-50 g/kg in 0.037a and of 50-60 g/kg in 0.037b were larger. Both LPI and COHESION were the largest in group 40-50 g/kg 0.037a and 0.037b. SHAPE-MN was largest in the group 30-40 g/kg in 0.037a and in the 40-50 g/kg in group of 0.037b.

SOM spatial distribution under sample-grid of 0.074 km^2: SOM spatial distribution trends varied among groups under the 0.074km^2. SOM was greater in the north and middle areas in 0.074a, and greater in the northwest and middle areas in 0.074b, the west edge region in 0.074c, the western area in 0.074d, and in the southwest area in 0.074e (Figs. 5a, b, c, d and e). TAs of 40-50 g/kg was largest in classes 0.074a, 0.074b, 0.074c, 0.074d and 0.074c, respectively, and the area of 60 g/kg >SOM> 40 g/kg accounts for 100%, 100%, 94%, 100% and 89% of the study area in 0.074a, 0.074b, 0.074c, 0.074d and 0.074c, respectively. Both NP and TP of 50-60 g/kg were largest in 0.074a, 0.074b and 0.074c, and 30-40 g/kg was the largest group in 0.074c, while NP was larger in 40-50 g/kg and TP was larger in 50-60 g/kg. Both LPI and COHESION of 40-50 g/kg were largest in classes 0.074a, 0.074b, 0.074c and 0.074e, while 50-60 g/kg was largest in class 0.074d. SHAPE-MNs of 40-50 g/kg was largest in classes 0.074b, 0.074c, 0.074d and 0.074e, while 50-60 g/kg was larger in 0.074a.

DISCUSSION

Soil nutrient spatial distribution was studied frequently in recent years, and the results were applied to fertility evaluation, formulated fertilization, regional nutrient management and so on. Generally, soil nutrient distribution was often simulated by geostatistical methods (interpolated by ordinary Kriging) (Wu et al. 2003, Liu et al. 2006, Sauer et al.

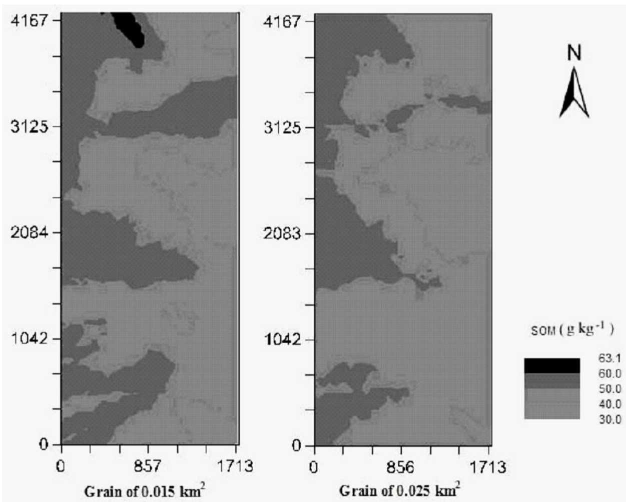

Fig. 3: SOM spatial distribution under grain of 0.015 km^2 and 0.025 km^2.

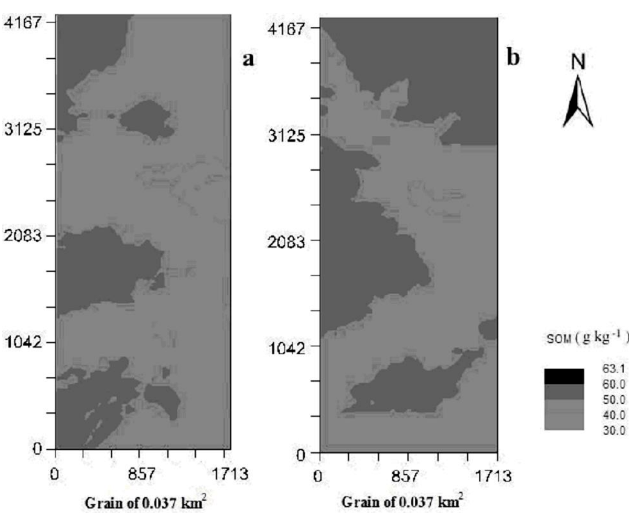

Fig. 4: SOM spatial distribution under grain of 0.037 km^2.

2006, Wei et al. 2006, Zhang et al. 2011, Fu et al. 2013, Liu et al. 2013). Before interpolation, the scatter of sample points should be uniformly spatially distributed, and the data need to fit to a normal distribution and second order stationary hypothesis. If the data do not fit to normal distribution, it should be converted by algebraic methods (ESRI 2010). In the study, Gaussian models were recognized as the best to predict SOM spatial distribution in all groups (Table 2). The proportion of the spatial structure (Nugget/sill, N/C) of <0.25, 0.25-0.75, and >0.75 can be used to describe strong, moderate and weak spatial autocorrelation, respectively (Zhang et al. 2007, Cambardella et al. 1994). Geostatistical results indicate that spatial autocorrelation as influenced by structure factors (e.g. climate, topography and so on) were moderate for 0.025 (0.50), 0.037b (0.41), 0.074a (0.50), 0.074c (0.45) and 0.074d (0.50), and strong for 0.015 (0.22), 0.037a (0.13), 0.074b (0.17) and 0.074e (0.16), respectively. Also, the relatively shorter autocorrelation distances (A_0) in groups were all close to 7 km under resolutions. These can conclude that sample resolutions can influence the analysis results of the spatial autocorrelations of SOM, but can not change the autocorrelation distances (A_0) which maybe mainly influenced by extent (research area). Generally, the interpolation maps by ordinary Kriging were similar between 0.015 and 0.025 (Fig. 3), and differed from 0.037a, 0.037b, 0.074a, 0.074b, 0.074c, 0.074d and 0.074e (Figs. 4 and 5). This indicates that a sample-grid ≤ 0.025km^2 was the best to fit to evaluate SOM spatial distribution in this watershed if the sample-grid method was adopted in a mollisol watershed of northeast China.

In the study area, the ranges of SOM contents were different when soil samples were grouped randomly. The value range of SOM content was largest in the 0.015 and 0.037b (221.7 g/kg), and was lowest in the 0.074c (53 g/kg), while the means of SOM (47.0 g/kg to 51.1 g/kg) were closer in each group (Table 6). Especially, the SOM means of 0.025 and 0.037b were close to that of 0.015, as well as standard deviation (SD) of 0.025 and 0.074d were close to that of 0.015, which also indicates that a sample-grid ≤0.025km^2 was the best to fit to evaluate SOM spatial distribution in this watershed if the sample-grid method was adopted in a mollisol watershed of northeast China.

At the same time, landscape indicators were also very effective to analyse the various spatial distribution of SOM under different resolutions. The areas of 60 g/kg>SOM> 40 g/kg account for 87% to 100% of the study area in all resolutions, and there was big difference when resolutions were different or soil sampling was different under the same resolution (Tables 3, 4 and 5). NP, TA, TP, LPI, SHAPE-MN and COHESION were different under different resolutions, e.g., NPs were higher at 40-50 g/kg, 50-60 g/kg, 50-60 g/kg and 40-50 g/kg in groups of 0.015, 0.025, 0.037a and 0.014b respectively, and were all lower at >60 g/kg in groups of 0.015, 0.025, 0.037a and 0.014b, respectively. TAs and COHESIONs were all higher at 40-50 g/kg in nine groups, and were all lower at >60 g/kg in nine groups, but the values in groups were different. NP, TA, TP, LPI, SHAPE-MN and COHESION were also different under groups in same resolution, e.g., in 0.074 resolutions, NPs were higher at 40-50 g/kg, 50-60 g/kg, 30-40 g/kg, 40-50 g/kg and 50-60 g/kg in groups of 0.074a, 0.074b, 0.074c, 0.074d and 0.074e respectively, and were all lower at >60 g/kg in 0.074 resolution groups. TAs and COHESIONs were all higher at 40-50 g/kg in nine groups except that in group of 0.074d for COHESION, and were all lower at >60 g/kg in

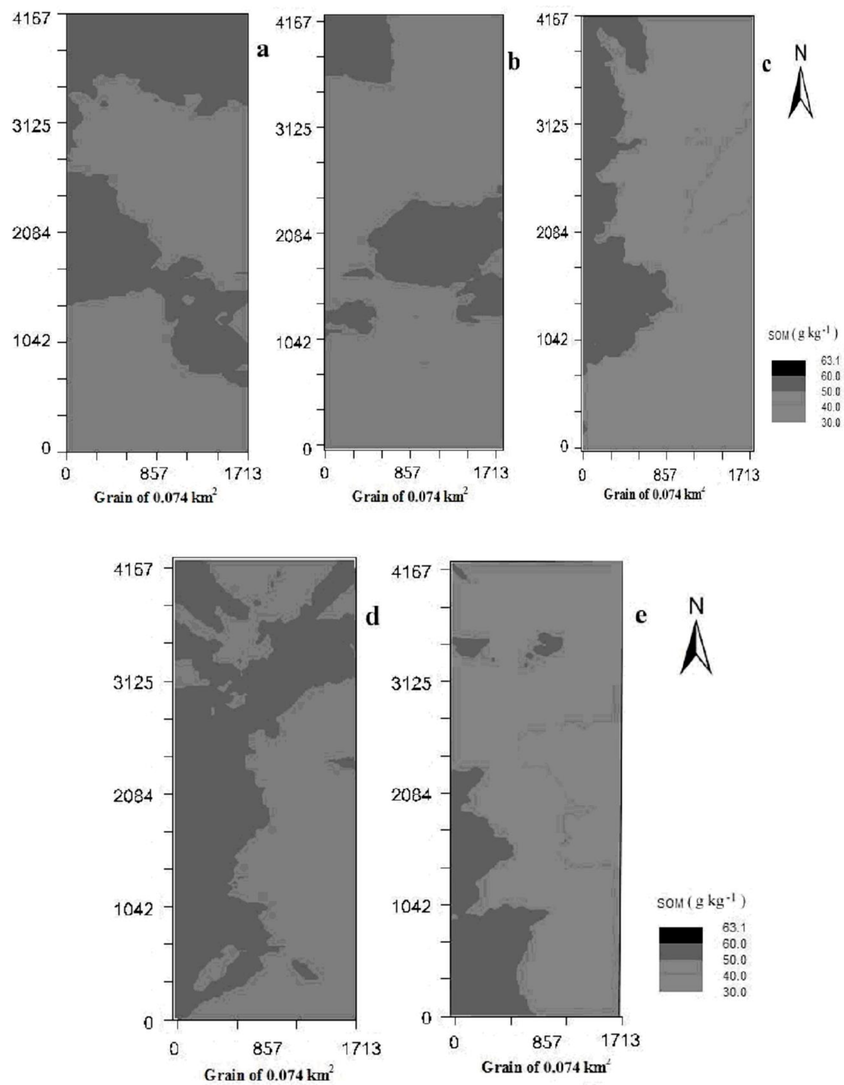

Fig. 5: SOM spatial distribution under grain of 0.074 km^2.

nine groups, and the values in groups were different too. However, both NP and TP of 40-50 g/kg or 50-60 g/kg in resolutions were larger, and most of LPI and COHESION of 40-50 g/kg were the largest in all groups, which indicated that the physical connectedness of the corresponding patch type of 40-50 g/kg or 50-60 g/kg was strongest in space under resolutions (Mc Garigal et al. 2012). SHAPE-MN showed that the degree of shape complexity was different among the data groups, and SHAPE-MN of 40-50 g/kg was greatest in groups 0.025, 0.037b, 0.074b, 0.074c, 0.074d, 0.074e, and 50-60 g/kg in data group 0.037a. Generally, the nutrient level of 40-50 g/kg in most resolutions was the most complex shape in classifications (Mc Garigal et al. 2012). In the study area, TA, LPI and COHESION of 0.015 resolution were relatively close to 0.025 resolutions, which also indicated that a sample-grid ≤ 0.025 km^2 was the best resolution to evaluate SOM spatial distribution in this watershed if a sample-grid method was adopted. These results also proved that the spatial pattern of SOM can be relatively well represented by the soil sampling with sample-grid ≤0.025 km^2, but can not be accurately predicted when sample-grid is higher than 0.025km^2.

In our study, soil sampling under different resolutions or in groups under the same resolution had an influence on the prediction of SOM spatial distribution by interpolating method (ordinary Kriging), despite the fact that all data were transformed by algebraic methods to fit a normal distribution, and cross-validation method with R^2 (Regression coefficient)

Table 3: Landscape indicators of soil organic matter (SOM) in the 0.015 km^2 and 0.025km^2 resolution.

Groups	SOM (g/kg)	NP	TA (km^2)	TP (km)	LPI (%)	SHAPE -MN	COHE-SION
	30-40	4	0.74	7725	7.3	1.41	99.00
0.015	40-50	6	3.41	25818	40.4	1.81	99.78
	50-60	2	2.22	2511	25.9	3.02	99.70
	>60	2	0.05	12754	0.8	1.22	97.36
	30-40	2	0.86	3030	12.4	1.47	99.45
0.025	40-50	2	4.00	4563	61.5	2.60	99.92
	50-60	7	1.59	49947	18.4	1.75	99.50
	>60	0	0	0	0	0	0.00

Table 4: Landscape indicators of soil organic matter (SOM) in the 0.037 km^2 resolution.

Groups	SOM (g/kg)	NP	TA (km^2)	TP (km)	LPI (%)	SHAPE -MN	COHE-SION
	30-40	2	0.24	5905	3.6	1.89	98.81
0.037a	40-50	9	4.55	64227	71.1	1.59	99.91
	50-60	10	1.51	44064	8.3	1.46	99.15
	>60	0	0	0	0	0	0
	30-40	2	0.07	9922	1.0	1.35	97.67
0.037b	40-50	1	3.60	638	56.4	3.02	99.92
	50-60	6	2.71	15875	19.9	1.45	99.57
	>60	0	0	0	0	0	0

Table 5: Landscape indicators of soil organic matter (SOM) in the 0.074 km^2 resolution.

Groups	SOM (g/kg)	NP	TA (km^2)	TP (km)	LPI (%)	SHAPE -MN	COHE-SION
	30-40	0	0	0	0		0
0.074a	40-50	6	3.94	22606	31.6	1.41	99.76
	50-60	5	2.55	35669	20.0	1.63	99.69
	>60	0	0	0	0	0	0
	30-40	0	0	0	0	0	0
0.074b	40-50	2	5.36	2954	78.3	1.69	99.96
	50-60	5	1.43	17260	13.8	1.50	99.41
	>60	0	0	0	0	0	0
	30-40	3	0.36	10866	5.4	1.41	99.05
0.074c	40-50	1	4.66	397	72.8	2.31	99.96
	50-60	2	1.38	7830	21.5	1.99	99.74
	>60	0	0	0	0	0	0
	30-40	0	0	0	0	0	0
0.074d	40-50	9	3.28	40562	40.0	1.64	99.66
	50-60	7	2.87	43421	42.0	1.57	99.81
	>60	0	0	0	0	0	0
	30-40	1	0.6502	873	11.20	1.76	99.31
0.074e	40-50	1	4.10	484	70.71	2.44	99.95
	50-60	6	1.05	34374	16.60	1.45	99.46
	>60	0	0	0	0	0	0

showed the estimated values fit well with the actual values (Table 2). This indicated that the accurate prediction of soil nutrient distribution was not only determined by sampling resolutions, but also mainly determined by the representative points of soil sampling which should reflect the soil characteristics, landscape, land use, and more information in the study area.

Table 6: Classical statistics parameters of SOM content in the watershed after interpolation.

Grain levels	Data group	SOM (g/kg) Mean	Max	Min	SD	Range
0.015	1,2,3,4,5	48.9	222.9	1.2	15.9	221.7
0.025	1,3,5	48.6	222.9	22.5	16.5	200.4
0.037a	1,4	50.3	147.6	24.6	14.5	123
0.037b	2,5	48.6	222.9	1.2	18.7	221.7
0.074a	1	49.5	86.6	26.8	13.2	59.8
0.074b	2	47.8	76.6	1.2	14.0	75.4
0.074c	3	47.0	80.3	27.3	11.6	53
0.074d	4	51.1	147.6	24.8	15.8	122.8
0.074e	5	49.4	222.9	22.5	22.6	200.4

CONCLUSIONS

Traditional statistics and geostatistical parameters together with landscape indicators were useful to analyse SOM spatial variability. Spatial autocorrelations as influenced by human activities were moderate for groups 0.025, 0.037b, 0.074a, 0.074c and 0.074d and strong for 0.015, 0.037a, 0.074b and 0.074e. The relatively shorter autocorrelation distances (A_0) in groups were all close to 7 km under all resolutions. SOM spatial distributions were similar between the 0.015 km^2 and 0.025 km^2 resolutions, but were different from other resolutions, despite that the data after transformation in group were close to normal distribution. Generally, a sample-grid ≤0.025 km^2 was recognized as a better resolution to predict SOM spatial variability by ordinary Kriging interpolation if a sample-grid method was adopted in the black soil region of northeast China, and the result needs to be proved in other regions. The accurate prediction of soil nutrient distribution was mainly determined by the representative points of soil sampling, which should reflect through resolution of the entire environmental factors in the research area.

ACKNOWLEDGEMENTS

Thanks to Valerie Kirkwood from Eastern Cereal and Oilseed Research Center, Agriculture and Agri-Food, Canada, Ottawa who edited this manuscript. Part of the paper is sponsored by the project of National Natural Science Foundation of China (41471228, 41101262) Heilongjiang Province Department of Education Program (12521010) and the Northeast Agricultural University (2012RCB03).

REFERENCES

Agassi, M., Morin, J. and Shainberg, I. 1990. Slope, aspect and phosphogypsum effects on runoff and erosion. Soil Science Society of America Journal, 54: 1102-1106.

Atreya, K.S., Sharma, R.M. and Bajracharya, N.P. 2008. Developing a sustainable agro-system for central Nepal using reduced tillage and straw mulching. Journal of Environmental Management, 88: 547-555.

Balasundram, S.K., Robert, P.C., Mulla, D.J. and Allan, D.L. 2006. Relationship between oil palm yield and soil fertility as affected by topography in an Indonesian plantation. Soil Plant Analysis, 37: 1321-1337.

Barton, A.P., Fullen, M.A. and Mitchell, D.J. 2004. Effects of soil conservation measures on erosion rates and crop productivity on subtropical Ultisols in Yunnan province, China. Agriculture Ecosysterm and Environment, 104: 343-357.

Cambardella, C.A., Moorman, T.B., Novak, J.M., Parkin, T.B., Karlen, D.L. Turco R.F. and Konopka A.E. 1994. Field-scale variability of soil properties in Central Iowa soils. Soil Science Society of America Journal, 58: 1501-1511.

DeBusk, W.F., Reddy K.R., Koch M.S. and Wang Y. 1994. Spatial distribution of soil nutrients in a northern Everglades marsh: Water conservation area 2A. Soil Science Society of America Joural, 58: 543-552.

Forman, P.T.T. 1995. Land mosaics: The Ecology of Landscape and Regions. Cambridge Univ. Press, Cambridge.

Fu, B.J., Chen, L.D., Ma, K.M. and Wang Y.L. 2011. Theory and application of landscape ecology. Science Press, Beijing, pp. 72-73.

Fu, W.J., Zhao, K.L., Tunney, H. and Zhang C.S. 2013. Using GIS and geostatistics to optimize soil phosphorus and magnesium sampling in temperate grassland. Soil science, 178(5): 240-247.

Gallardo, A. 2003. Spatial variability of soil properties in a floodplain in Northwest Spain. Ecosystems, 6: 564-576.

Gardner, R.A.M. and Gerrard A.J. 2003. Runoff and soil erosion on cultivated rainfed terraces in the middle hills of Nepal. Appl. Geogr., 22: 23-45.

Heilongjiang Bureau of Land Management 1992. Soils in Heilongjiang province, China Agriculture Press, Beijing, pp. 166-170.

Horn, R., Dom, H., Sowi ska-Jurkiewicz, A. and Ouwerkerk, C. Van 1995. Soil compaction processes and their effects on the structure of arable soils and the environment. Soil Tillage and Research, 35(1-2): 23-36.

Huang, C.Y. 2000. Soil Science. China Agriculture Press, Beijing.

Isaaks, E.H. and Srivastava, R.M. 1989. Applied Geostatistics. Oxford University Press, New York.

Lal, R. 1998. Soil erosion impact on agronomic productivity and environmental quality. Critical Reviews in Plant Sciences, 17: 319-464.

Lal, R. 2004. Soil carbon sequestration impacts on global climate change and food security. Science, 304: 1623-1627.

Li, X.X., Shao, Y. and Jiang L.N. 2008. Biostatistics. Science Press, Beijing.

Liu, Z.P., Shao, M.A. and Wang, Y.Q. 2013. Spatial patterns of soil total nitrogen and soil total phosphorus across the entire Loess Plateau region of China. Geoderma, 197-198: 67-78.

Liu, D., Wang, Z., Zhang, B., Song, K., Li, X., Li, J., Li, F. and Duan, H. 2006. Spatial distribution of soil organic carbon and analysis of related factors in croplands of the black soil region, northeast China. Agriculture, Ecosysterm and Environment, 113: 73-81.

McGarigal, K., Cushman, S.A. and Ene, E. 2012. FRAGSTATS v4: Spatial Pattern Analysis Program for Categorical and Continuous Maps. Computer software program produced by the authors at the University of Massachusetts, Amherst. Available at the website: (http://www.umass.edu/landeco/research/fragstats/fragstats.html).

Morgan, R.P.C. 2005. Soil Erosion and Conservation, 3rd edn. Blackwell Publishing Ltd., USA.

Moulin, A.P., Anderson, D.W. and Mellinger M. 1994. Spatial variability of wheat yield, soil properties and erosion in hummocky terrain. Canadian Journal of Soil Science, 74: 219-228.

Noorbakhsh, S., Schoenau, J., Si, B., Zeleke, T. and Qian, P. 2008. Soil properties, yield, and landscape relationships in south-central Saskatchewan. Canada Journal of Plant Nutrition, 31: 539-556.

Oliver, M.A. 1987. Geostatistics and its application to soil science. Soil Use and Management, 3(1): 8-20.

Oliver, M.A., Webster, R. and Slocum, K. 2000. Filtering SPOT imagery by kriging analysis. Journal of Remote Sensing, 21(4): 735-752.

Park, S.J. and Lekm, G.V. 2002. Environmental correlation of three-dimensional spatial soil variability: A comparison of three adaptive techniques. Geoderma, 109: 117-140.

Rundel, P.W. 1981. The matorral zone of central Chile. In: di Castri F., Goodall, D.W. and Spetch, R.L. (eds) Mediterranean Type Shrublands. Elsevier, Amsterdam, pp. 175-201.

Sauer, T.J., Cambardella, C.A. and Meek, D.W. 2006. Spatial variation of soil properties relating to vegetation changes. Plant Soil, 280: 1-5.

Silveira, M.L., Comerford, N.B., Reddy, K.R., Prenger, J. and Debusk, W.F. 2009. Soil properties as indicators of disturbance in forest ecosystems of Georgia, USA. Ecological Indicator, 9(4): 740-747.

Soil Survey Service of Hailun 1985. Soil science of Hailun journal. Heilongjiang Press, Harbin.

Turner, M.G., O'Neill, R.V. and Gardner, R.H. 1989. Effects of changing spatial scale on the analysis of landscape pattern. Landscape Ecology, 3(4): 153-162.

Van Doren, C.A., Stauffer, R.S. and Kidder, E.H. 1950. Effect of contour farming on soil loss and runoff. Soil Science Society of America journal, 15: 413-417.

Verity, G.E. and Anderson, D.W. 1990. Soil erosion effects on soil quality and yield. Canadian Journal of Soil Science, 70: 471-484.

Voroney, R.P., van Veen, J.A. and Paul, E.A. 1981. Organic C dynamics in grassland soils. 2. Model validation and simulation of the long-term effects of cultivation and rainfall erosion. Canadian Journal of Soil Science, 61: 211-224.

Walson, D.A. and Laflen, J.M. 1986. Soil strength, slope and rainfall intensity effect on interrill erosion. Trans ASAE, 29: 98-102.

Wei, J., Xiao, D., Zhang, X., Li, X. and Li, X. 2006. Spatial variability of soil organic carbon in relation to environmental factors of a typical small watershed in the black soil region, northeast China. Environmental Monitor Assessment, 121: 597-613.

West, T.O. and Post, W.M. 2002. Soil organic carbon sequestration rates by tillage and crop rotation: A global data analysis. Soil Science Society of America Journal, 66: 1930-1946.

Wu, J., Norvell, A., Hokins, D.G., Smith, D.B., Ulmer, M.G. and Welch, R.M. 2003. Improved prediction and mapping on soil copper by kriging with auxiliary data for cation-exchange capacity. Soil Science Society of America Journal, 67: 919-927.

Yost, R.S., Uehara, G. and Fox, R.L. 1982. Geostatistical analysis of soil chemical properties of large land areas. II. Kriging. Soil Science Society of America Journal, 46: 1033-1037.

Zhang, X.Y., Sui, Y.Y., Zhang, X.D., Meng, K. and Herbert, S.J. 2007. Spatial variability of nutrient properties in black soil of Northeast China. Pedosphere, 17(1): 19-29.

Zhang, S.L., Zhang, X.Y., Huffman, T., Liu X.B. and Yang J.Y. 2011. Influence of topography and land management on soil nutrients variability in Northeast China. Nutrient Cycling in Agroecosysterms, 89: 427-438.